*Journal of Thermal Analysis, Vol. 36 (1990) 331-359*

*Invited Review*

# THERMALLY STIMULATED LUMINESCENCE AND CONDUCTIVITY - ADDITIONAL TOOLS FOR THERMAL ANALYSIS OF POLYMERS

*R. J. Fleming*

INSTITUTE FOR MOLECULAR SCIENCE OKAZAKI, JAPAN 444*

(Received May 31, 1989)

The physical phenomena underlying thermally stimulated luminescence and conductivity measurements, logically considered as complementary to conventional thermal analysis measurements, are outlined. The equipment and samples required to make such measurements are briefly described, and the basic concepts underpinning the interpretation of the data sketched. Some recent experimental data, chosen to reflect the sensitivity of thermally stimulated luminescence and conductivity to doping of the sample and changes in its morphology, are presented and discussed.

The application of thermal analysis techniques to the study of organic polymers has increased rapidly in recent years [1, 2]. The range of information which can be extracted from such measurements is impressive, e.g. glass transition, crystallization and melting temperatures, the effects of additives such as plasticizers and stabilizers on these parameters, thermal stability, degree of curing, and possibly identification of the components in a polymer mixture.

---

*Permanent Address: Department of Physics Monash University Clayton, Victoria 3168 Australia

*John Wiley & Sons, Limited, Chichester*
*Akadémiai Kiadó, Budapest*

The accuracy and flexibility of modern commercial thermal analysis instrumentation, boosted by computer-controlled data acquisition and processing, have increased the popularity of these techniques. However, they are macroscopic techniques, in the sense that the data obtained is interpretable only in terms of the bulk properties of the samples, not at the atomic or electronic level.The purpose of this article is to describe and discuss some of the information which may be extracted from thermally stimulated luminescence (TSL) and thermally stimulated conductivity (TSC) measurements on polymers. Such measurements may logically be considered as forms of thermal analysis in the sense that the phenomena of interest are triggered simply by heating the sample; however, electrical polarization and/or exposure to some form of ionizing radiation before heating are also necessary. These measurements are straight-forward experimentally, and less dependent than DTA/DSC measurements on the "correct" choice of experimental conditions, e.g. ambient gas pressure, heating-rate, sample size. The necessary equipment is inexpensive, and TSL measurements in particular are very sensitive, i.e. very low light levels can be measured and so very small concentrations of trapped electrons and impurity luminescence centres can be detected. There are of course limitations ; TSL emission in many commercial polymers is negligible above room temperature, and the information which can be extracted from a single TSL or TSC measurement on the molecular environment of the trapped electrons is not as precise as that from, say, a single ESR scan. In order to facilitate a more precise interpretation it is therefore essential to investigate changes in the TSL/TSC data resulting from various treatments of the sample, e.g. annealing at several temperatures, exposing to a strongly oxidising environment, immersing in an organic solvent such as hexane. There is also considerable benefit to be derived from making simultaneous TSL/TSC measurements on the same sample, as in conventional thermal analysis measurements [3].

## The origins of TSL and TSC

### *TSL*

TSL (or thermoluminescence TL) is the name commonly given to the emission of visible and/or ultra-violet light when a sample, having been exposed to some form of ionizing radiation, is heated. It should not be confused with chemiluminescence, which is the emission of light originating in a chemical reaction [4]. TSL is observable in most dielectrics; in polymers the sample is commonly irradiated at liquid nitrogen temperature and heated to room temperature at a rate of approximately 3 deg/min. The radiation generates throughout the sample volume a uniform concentration of electron-ion pairs, some of which do not recombine but separate, yielding a trapped electron localized in a potential well and an immobile or very slowly moving luminescence centre ion. The electron escapes from its trap when the sample is heated, and recombines with its geminate luminescence centre or some other more distant luminescence centre to re-form the original molecule in an excited state. The decay of the excited state to the ground state, if radiative, generates TSL.

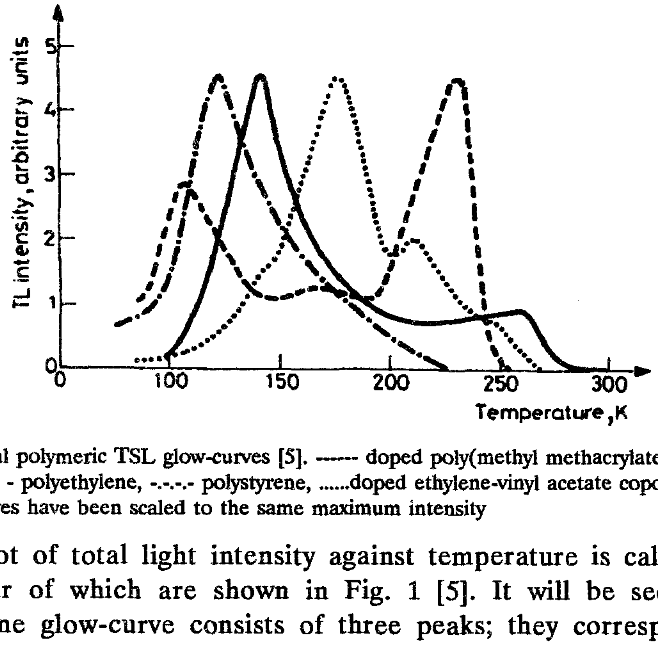

Fig. 1 Typical polymeric TSL glow-curves [5]. ------ doped poly(methyl methacrylate), - - - - polyethylene, -.-.-.- polystyrene, ......doped ethylene-vinyl acetate copolymer. The curves have been scaled to the same maximum intensity

The plot of total light intensity against temperature is called a glow-curve, four of which are shown in Fig. 1 [5]. It will be seen that the polyethylene glow-curve consists of three peaks; they correspond to the onset of various types of molecular motion within the polymer, namely, in order of increasing temperature, oscillatory/rotational motion of short side-chains attached to the main chain, "crank-shaft" motion of short main-chain segments between sterically-permitted configurations, and the glass transition, all in the amorphous regions of the sample [6]. Thus TSL complements DTA/DSC inasmuch that both can detect polymeric molecular motion. The TSL spectra for samples of four common polymers appear in Figure 2. In the relatively few polymer samples where the luminescence centres have been convincingly identified they have turned out to be impurity molecules unintentionally incorporated during commercial processing or in research laboratory synthesis (see under Luminescence Centres).

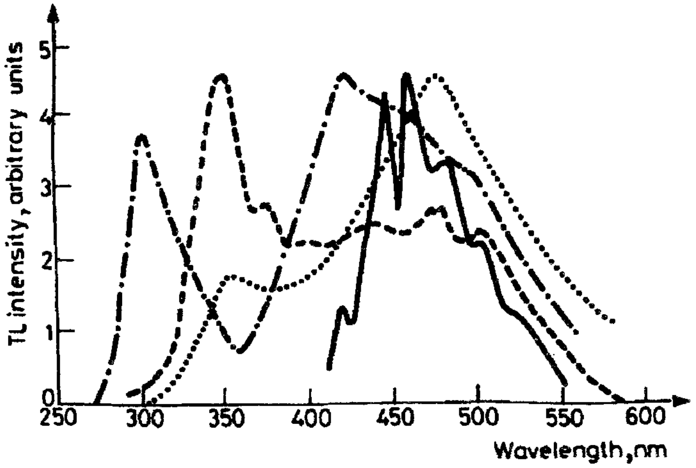

**Fig. 2** Typical polymeric TSL emission spectra [5]. -----doped poly(methyl methacrylate), - - - - polymethylene, -.-.-.- polystyrene, ..... poly(ethylene terephthalate). The curves have been scaled to the same maximum intensity

## *TSC*

TSC may be considered as the electrical analogue of TSL, in that a current rather than light intensity is measured while the sample is being heated. However there is some inconsistency in the literature over the use of the term TSC. The measurements usually reported may be divided into two main categories: -

(1) A strong dc electric field (typically $10^5$ V/cm) is applied to the sample for about 30 min, usually at room temperature in the case of polymers. This is the polarization process. The sample is then cooled (say to liquid nitrogen temperature) with the field still applied, and heated in short-circuit, usually without any prior exposure to radiation. The current measured during heating originates in

(a) disorientation of dipoles with significant dipole moment, previously oriented by the applied field, and/or

(b) movement under its self-field of charge (electronic) injected into the sample by the applied field, or movement of pre-existing charge (electronic or ionic) under the same field. This current is therefore most appropriately

described as thermally stimulated depolarization (TSD) current, in the sense that it originates in processes which occur while the sample is returning to its equilibrium state from its polarized state. Alternatively the sample may be cooled before the polarizing voltage is applied, in which case the current measured during heating with the field still applied is usually called thermally stimulated polarization (TSP) current. Such a current may also have dipole and injected charge components, in the opposite sense to the corresponding TSD components, and a displacement component originating in changes in sample dimensions and relative permittivity with temperature.
(2) The sample is polarized and cooled as in the TSD procedure, but is then exposed to a source of ionizing radiation and heated with the external field still applied. The purpose of the radiation is to generate a uniform concentration of trapped electron/ion pairs throughout the sample volume, as in TSL measurements. Since the field is still applied during heating there will be no dipole contribution to the current measured during heating, since the dipoles will retain their oriented configurations under the influence of the field. The additional role of the field is to oppose the Coulomb attraction between electron and ion, so that some of the electrons do not recombine with the nearest ion but drift some distance under the influence of the field before recombining with another ion or being collected at the anode. (In the absence of an applied voltage as many electrons will move from left to right to recombine with an ion as move from right to left, giving zero net current.) If the field is applied before cooling, removed during irradiation and re-applied during heating, and the resulting current compared with that measured with the field applied continuously during the experiment, the influence of the field on the yield of charge carriers from the irradiation may be studied. In either case the current measured during heating is appropriately labelled as TSC current, since it originates mainly in the conduction of electrons through the sample bulk. It will have a small displacement component which can be measured by heating the sample without prior irradiation, but in polymers this component is usually negligible for the doses commonly employed.

The essential difference between TSD and TSC measurements is that in the latter the sample is exposed to some form of ionizing radiation, or corona discharge, before heating. This distinction will be maintained throughout the remainder of this paper.

A TSD plot for a poly(methyl methacrylate) sample polarized at 120° and a field strength of $2\times10^4$ V/cm is shown in Figure 3 [7]. The $\rho$-peak is attributed to the migration of pre-existing ionic charge, and the other three

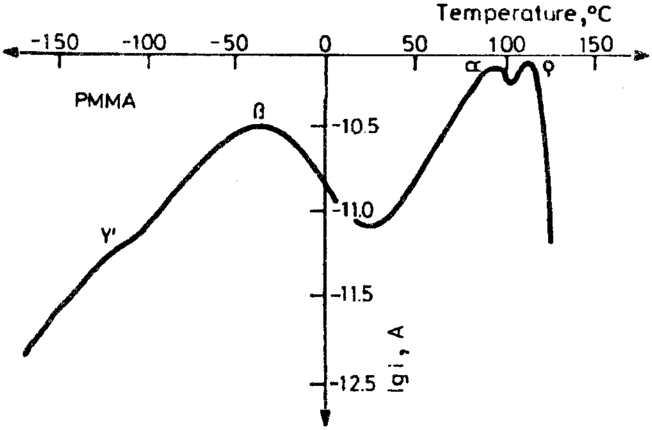

Fig. 3 TSD current plot for poly(methyl methacrylate) [7]. The sample was polarized at 393 K at a field strength of $2.10^4$ V/cm. The peaks are attributed to ionic migration ($\rho$), co-operative motion of side-groups and backbone segments around the glass transition ($\alpha$), motion of side-groups alone ($\beta$), and motion of absorbed water molecules ($\gamma$)

peaks to dipole disorientation triggered by the onset of various kinds of molecular motion, i.e. (i.) $\alpha$-peak; motion of dipolar side-groups attached to large segments of the back-bone, occurring around the glass transition, (ii) $\beta$-peak; motion of side-groups alone, and (iii) $\gamma'$-peak; motion of absorbed water molecules [7, 8]. In general the only motion possible within polymers at low temperature is highly localized, e.g. rotation of side-groups or intra side-group motion, while at higher temperatures segments of the main chain backbone become mobile at the glass transition.

The magnitude of the TSD current measured for a given sample will obviously depend on the dipole moment of the orienting dipoles and the strength of the polarizing field. A nominally non-polar polymer such as polyethylene should not yield any dipole current, but the unintentional incorporation of polar impurities such as C=O groups during commercial processing leads typically to a current of order $10^{-13}$ A in a sample with an electrode cross-sectional area of 5 $cm^2$ polarized at room temperature at a field strength of $10^5$ V/cm, and heated from liquid nitrogen temperature.

A TSL glow-curve and a TSC plot measured simultaneously on a low density polyethylene sample are shown in Figure 4 [9]. Note the correlation between the two lower temperature peaks in each plot, and the fact that although the TSL intensity falls rapidly above about -30°, due to the decreasing probability of radiative recombination with increasing temperature, the TSC current increases by a factor of almost $10^2$ between -30° and 0° (and indeed continues to increase up to the melting point) due to the glass transition and enhanced charge carrier injection and mobility. Thus TSC is not subject to the same upper temperature limitations as TSL.

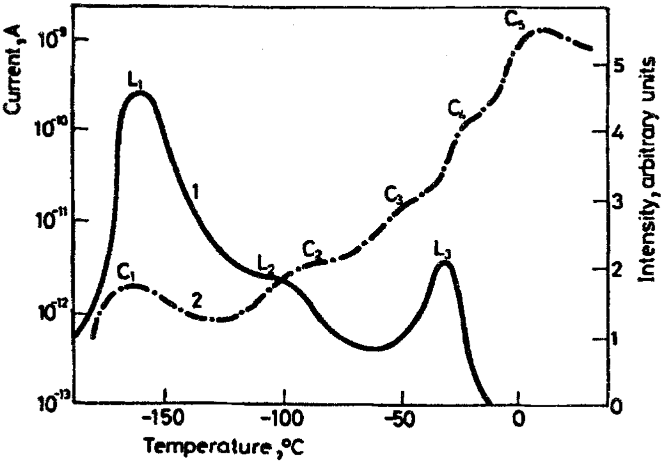

**Fig. 4** Simultaneous TSL (1) and TSC (2) in low density polyethylene [9]

The minimum irradiation dose, absorbed at liquid nitrogen temperature, required to yield a workable TSL signal is of order 100 Gy for most polymers, assuming a sample thickness around 100 $\mu$, an irradiated area of 5 $cm^2$ and a mid-range sensitivity photomultiplier with a cooled photocathode coupled to a photon counter. Even at an applied field strength of $10^5$ V/cm, the minimum dose required for a workable TSC current (say $> 10^{-13}$A) in a sample of the same dimensions is at least fifty times greater. The difference originates in the fact that, despite the applied voltage, a large majority of the trapped electrons combine with the nearest luminescence centre ion (usually their parent molecule in polymers) under the influence of their mutual Coulomb attraction, the symmetrical distribution of their separations generating zero net current, as described above.

Clearly TSD/TSL/TSC are valuable techniques in fundamental research on dipole motion, on trapping, storage and transport of charge in dielectrics, and on the response of these materials to ionizing radiation.

They have a place too in the applications area, arising mainly from their ability to monitor charge storage. Thus TSL is widely used for radiation dosimetry, e.g. personnel dosimetry, environmental monitoring, radiation therapy and particulate radiation dosimetry [10]. The applications of TSC/TSD are mainly in connection with the stability of the electret (in some ways the electrical analogue of the magnet), e.g. earphones and microphones, gas filters, relay switches and optical switches, and in electrophotography [11].

## Equipment

The apparatus required for TSL/TSD/TSC studies is relatively simple and inexpensive. A typical vacuum cell for simultaneous measurements on the same sample, from liquid nitrogen temperature up to about 220°, is shown in Fig. 5 [9]. Note that the sample is heated (and cooled) from both sides in order to reduce temperature gradients as much as possible. The usual sample thickness is in the range 25 $\mu$m-1 mm. The thinner the sample the better for TSD/TSC measurements, since strong electric fields can then be generated within its volume without applying very high voltages; on the other hand one would expect the TSL intensity to be linearly proportional to sample thickness, assuming uniform irradiation, but self-absorption and limited transparency can sometimes lead to a sub-linear dependence or independence. Since TSL detection using a photomultiplier with a cooled photocathode is usually much more sensitive than current measurement using a state-of-the-art electrometer, the choice of sample thickness is normally governed by current measurement considerations. The irradiated surface of the sample carries an evaporated electrode (frequently gold) about 100 nm thick, the electrode on the other surface being not more than roughly 30 nm thick (semi-transparent) so that it will allow adequate TSL transmission but still function satisfactorily as an electrode. The lead-glass window in the photomultiplier port prevents ionizing radiation from damaging the photomultiplier, but may also absorb the TSL emission non-uniformly, thereby distorting the spectrum. An alternative solution is to insert a lead shutter in the photomultiplier port which can be opened after irradiation, but this requires a vacuum-tight/light-tight flexible coupling. To measure the TSL spectrum a monochromator is inserted between the cell and the photomultiplier, and the appropriate wavelength range is scanned as quickly as possible at the temperature of interest. The resulting spectrum must then be corrected for variation of total intensity during the scan. This is most conveniently done by recording the total intensity in a previous run and taking care to maintain the same heating rate during the spectral scan.

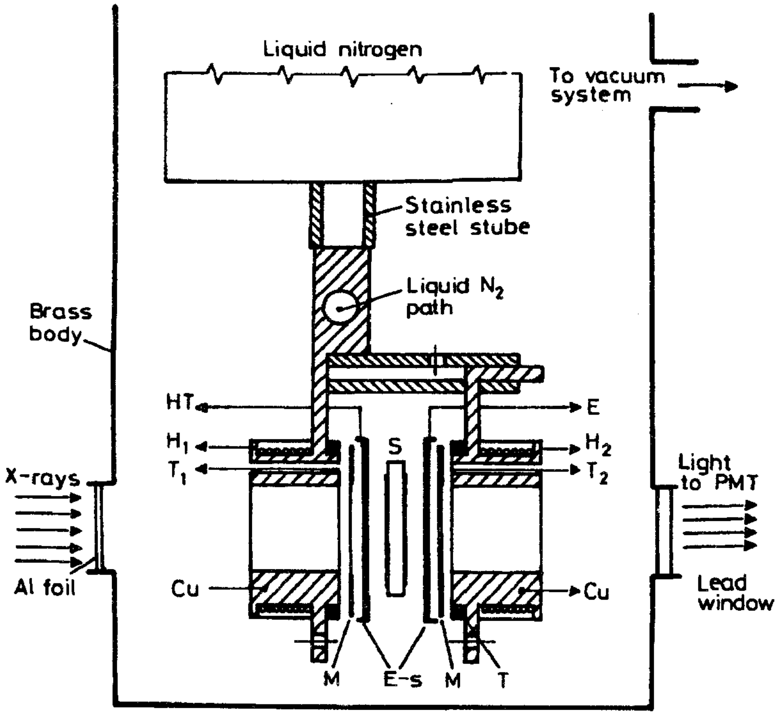

Fig. 5 A schematic diagram of a cryostat for simultaneous TSL/TSC measurements [9]. $T_1$, $T_2$-thermocouples; $H_1$, $H_2$-heaters; HT-power supply; E-electrometer, T-Teflon; M-Mylar sheets; E-s-gold-plated copper electrodes; S-sample with evaporated gold electrodes (one semitransparent)

## Dipolar depolarization

We outline briefly now the mathematics of the dipole depolarization process, and calculate the associated external current observed in TSD measurements.

In the simplest case, the decay of the polarization when the sample is short-circuited is given by

$$P(t) = P_o \exp(-t/\tau) \qquad (1)$$

where $P(t)$ is the polarization at time $t$ after short-circuiting, $P_o$ is its value at $t = 0$, and $\tau$ is the dipolar relaxation time. We are assuming that all the dipoles have the same $\tau$. The depolarization current density $J(t)$ is then

$$J(t) = -\mathrm{d}P(t)/\mathrm{d}t = P(t)/\tau \qquad (2)$$

Now $\tau$ is a function of temperature $\tau(T)$, and for a constant heating rate $q$ commencing at the polarization temperature $T_o$ we have

$$T = T_o + qt \qquad (3)$$

Equation (1) may then be re-written in the form

$$P(T) = P_o(T_o) \exp\left(-\int_{T_o}^{T} \mathrm{d}T'/\tau(T')\right. \qquad (4)$$

Assuming

$$\tau(T) = \tau_o \exp(E/kT) \qquad (5)$$

where $\tau_o$ is the relaxation time at infinite temperature, $E$ is the activation energy of the motion which triggers the dipole disorientation and k is Boltzmann's constant, combining Eq. (2-5) we obtain

$$\begin{aligned} J(T) &= (P_o(T_o)/\tau_o) \exp(-E/kT)) \\ &\exp[-(q\tau_o)^{-1}\int_{T_o}^{T} \exp(-E/kT'))\,\mathrm{d}T'] \end{aligned} \qquad (6)$$

Equation (6) describes a single TSD peak, in which the first exponential factor on the R.H.S. controls the initial rise of the current, and the second controls the subsequent maximum and fall off to zero. In other words the rapidly increasing mobility of the dipoles with increasing temperature causes the current to increase, and the decreasing number of dipoles remaining oriented eventually causes it to decrease.

In practice the sample may well contain a distribution of activation energies, or relaxation times, or both, generating a single current peak. Adjacent peaks may also overlap, as shown in Fig. 3. Discussion of the literature on the analysis of complex TSD current plots, which are closely related to dielectric loss plots, is inappropriate here. Reference [7, 8] are recommended to the interested reader.

## Trapping and release of electrons

In this Section we consider various aspects of the electron trapping and release processes.

### *Trap structure*

Four types of electron trap seem likely in polymers:

(a) Cavity traps, which are voids resulting from the local spatial configurations of the chains in the amorphous regions of the sample [12]. Such traps disintegrate with the onset of some form of local molecular motion, leaving the electrons free to move.

(b) Neutral molecules with a positive electron affinity, e.g. molecular oxygen [12]. The TSL glow-curves of several common polymers certainly alter shape quite dramatically when absorbed gases are pumped out. Some recent work on low density polyethylene [6] suggests that the traps are not simply the gas molecules themselves, but some loosely bound complexes formed by them in association with the polymer matrix. Note that such traps are unlikely in the crystalline regions, whose dense molecular packing renders them essentially impermeable to nearly all gases.

(c) Free radicals [12]. These would certainly be expected to capture electrons, but a convincing temperature correlation between ESR absorption intensity and TSL intensity or TSC current in a polymer does not seem to have been demonstrated to date. Radicals have been shown to act as luminescense centres in doped poly(methyl methacrylate) [13, 14].

(d) Various types of defects within the crystalline regions [9], e.g. vacancies, kinks, or chain ends formed during rapid crystallization. Such traps would be "normal" in the sense that electrons would escape from them on absorbing sufficient energy from the surroundings, rather than when the traps were broken up by molecular motion, as in the case of cavity traps. Total trap concentrations, which very few authors have estimated, vary considerably between samples, but a figure of $10^{17}$-$10^{18}$ $cm^3$ (in polymers) is mid-range [15].

*Activation energies and frequency factors*

The two parameters which are usually evaluated for a given peak in a TSL or TSC glow-curve are the frequency factor and the trap depth or activation energy. Considering a model of an electron trapped in a stable cylindrical potential well, the activation energy is simply the depth of the well and the frequency factor is the product of the number of times per second the electron collides with the walls of the well and an entropy factor related to possible changes in the lattice configuration in the neighbourhood of the trap when the electron escapes. Randall and Wilkins [16] wrote

$$R(T) = n(T)\, s(T)\, \exp(-E/kT) \tag{7}$$

where $R(T)$ is the rate of escape of electrons from traps, $n(T)$ is the trapped electron concentration, and $s(T)$ and $E$ are respectively the frequency factor and activation energy as described above. Development of Eq.(7) to give the variation of TSL or TSC when the sample is heated yields an expression essentially identical to Eq.(6), and may be found in [17]. $s(T)$ is expected to be a slowly varying function of temperature, but most authors take it as constant over a single glow-curve peak.

A study of TSL in polystyrene [18] showed a quasi-continuous distribution of activation energies covering the range 0.05-0.45eV, $s(T)$ increasing from 10 at 77K to $10^6$ at 250K; the distribution of activation energies, rather than a few discrete values, suggests that the associated traps were of the cavity type. Creswell and Perlman [19] made TSD measurements on Mylar (poly(ethylene terephthalate)) samples corona-charged at room temperature and reported four current peaks between 313 and 413K, for which they deduced activation energies of 0.55, 0.85, 1.4 and 2.2eV (all +/- 0.1eV). The two lower peaks were associated with trapped electrons or holes, and the upper two possibly with ionic trapping. The corresponding frequency factors were approximately $10^5$, 10, $10^{-6}$ and $10^{-16}$ $s^{-1}$ respectively. The authors suggested that the very low frequency factor calculated for the deepest trap might indicate an interfacial trap or perhaps some form of complex.

Many authors have developed methods for extracting $E$ and $s(T)$ values from glow-curves. Some require only the substitution of values for parameters such as peak temperature, width at half-height and form factor (a measure of the asymmetry of the peak) in simple equations, while others involve variation of the heating-rate or analysis of the initial rise of the luminescence or current. In this article we shall not be concerned with the details of these methods; an excellent summary is given in [17].

### *Escape mechanisms*

The following mechanisms for electron escape from traps have been proposed:

(a) Thermal excitation over the top of the stable potential barrier presented by the trap [16]. This is the most commonly envisaged mechanism, applicable to any solid sample.

(b) Thermal erosion of the traps, at temperatures below the melting point [12]. This mechanism is probably appropriate only for cavity traps in the amorphous regions of polymers, as mentioned above. The activation energies deduced from TSL/TSC measurements are not then the depths of the potential wells (cavities) but the energies required to initiate the appropriate molecular motion. Such motion is frequently detectable by DSC, dielectric or dynamic mechanical loss. The activation energies deduced from TSC/TSL measurements should then be identical with those from TSD measurements, and $s(T)$ should correspond to the inverse of the dipolar relaxation time $\tau(T)$

(c) Tunnelling through the potential barrier separating the electron from a nearby luminescence centre [20-22]. Observations which favour tunnelling but which are not necessarily inconsistent with escape via thermal excitation are [20]:-

(1) Isothermal decay of TSL of the form $I(t) = At^{-m}$, where $A$ is a constant and $m$ is close to unity,

(2) TSL intensity after irradiation at 13K not much less than after irradiation at 77K,

(3) Very little reduction in TSL intensity when the temperature was rapidly reduced from 50K to 16K. Appropriate parameters such as the width of the barrier through which the electron tunnels and the initial electron/luminescence centre separation are not accurately known, and so the numerical credibility of this model is difficult to assess.

The Randall and Wilkins mathematical analysis of charge release from traps [16] can be applied to both the thermal excitation and trap disintegration models. However, since the glass transition in the amorphous regions and melting in the crystallite regions of a polymer involve a large increase in the amplitude of the chain motion over a narrow temperature range, it is widely believed that one cannot analyse these processes in the terms of thermal activation, e.g. Eq.(7). (See however Bernes *et al* [23].) The glass transition is well described by the semi-empirical Williams-Landel-Ferry equation

$$\alpha(T) = \alpha_o \exp[C_1(T - T_g)/(C_2 + T - T_g)] \quad (T > T_g) \qquad (8)$$

where $\alpha(T)$ is the relaxation frequency of the motion associated with the glass transition at temperature $T$, $T_g$ is the glass transition temperature, and $\alpha_o$, $C_1$ and $C_2$ are "universal" constants. This equation is valid over the approximate range $T_g$ to $T_g + 50$ [24-25].

### Luminescence centres

The TSL spectrum of a given polymer may contain both fluorescent and phosphorescent components [26]. Fluorescent transition probabilities vary very little with temperature, unlike their phosphorescent counterparts which decrease with increasing temperature mainly because the probability of collisional deactivation of the excited state increases [27]. One must therefore expect a priori that the TSL spectrum of a given sample will alter during heating; there may also be more than one luminescence centre. It has been reported that the TSL spectra of polyethylene, isotactic polypropylene, poly(ethylene terephthalate) and polystyrene shift towards longer wavelengths with increasing temperature between 77K and room temperature, and also with increasing radiation dose at 77K [28-30]. The authors attributed the shift with increasing temperature to electron escape from deeper traps, but change in the vibrational energy spectrum of the luminescence centres would seem to be a more likely explanation. The shift with increasing dose could be due to ionization of all low concentration luminescence centres at lower doses.

Few authors have identified the luminescence centres. Charlesby and Partridge [31] measured the spectra of polyethylene, polystyrene, polypropylene and polytetrafluoroethylene and concluded that in each case the emission originated within a carbonyl group. This finding has been confirmed for polystyrene [18]. Boustead and Charlesby [32] suggested that the luminescence centres in the amorphous regions of polyethylene are free molecules of anthracene and phenanthrene, along with a naphthalene derivative attached to the chains; in the crystalline regions they suggested benzoic acid and aryl-alkyl ketones. Allen *et al.* [33] investigated low density polyethylene, one batch of samples having been prepared using molecular oxygen as a polymerization initiator, and another using a benzoyl compound. They attributed the fluorescence component of the photoluminescence spectrum of both batches to an $\alpha,\beta$-unsaturated carbonyl group of the enone type, and the phosphorescence components of the oxygen- and benzoyl-initiated batches to a dienone and benzoic acid respectively. They found no evidence of polynuclear aromatic luminescence centres.

A confident identification of the luminescence centres in a given polymer sample is not easy, mainly because the spectrum will probably consist of several partially overlapping components. However, it is in principle possible to detect very small impurity concentrations in this non-destructive manner.

## Recent data

We consider now some recent data, chosen to show the sensitivity of TSL/TSC/TSD measurements in polymers to morphological changes and doping.

### *TSL*

(a) Aulov *et al.* [34] investigated the effects of uniaxial stretching on the TSL of linear low density polyethylene gammairradiated at 273K in air. Glow-curves for three stretched samples of different molecular weight are shown in Fig. 6. Since the TSL intensity could be greatly reduced by exposing the samples to the light from an incandescent filament before heating, and no TSL was detected below 373K in unirradiated stretched and unstretched samples, the authors deduced that the TSL originates in the release of trapped charge generated by the irradiation. They also suggested that the release is triggered by vibrational/re-orientational chain motion between and within crystallites. Other salient observations were:

(i) The intensity of the TSL maximum varied little with the "multiplicity of

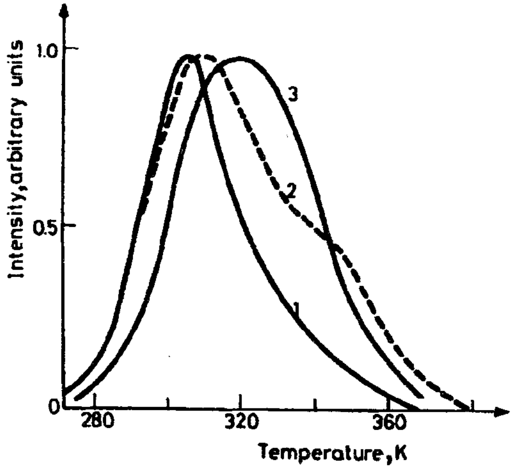

**Fig. 6** TSL glow-curves of three stretched polyethylene samples gamma-irradiated in air at 273K. The molecular weight of the samples increased from sample 1 to sample 3 [34]

stretching" $\mu$ for $1 < \mu < 10$ , but then increased rapidly up to $\mu = 30$. ($\mu$ is not defined specifically in the paper, but is presumably proportional to the increase in length.) There were considerable intensity differences between the three samples of different molecular weight at the same $\mu$ value.

(ii) Annealing for 30 minutes at 400K reduced the maximum intensity to approximately 10% of that for an un-annealed sample. The intensity was not affected by annealing below 330K.

(iii) The longitudinal dimension of the crystallites increased monotonically with $\mu$, while their transverse direction, the value of the long period and the % crystallinity varied little for $\mu > 10$.

(iv) Immersion of the samples in hexane and carbon tetrachloride had little effect on the TSL intensity.

The authors suggest that, for $\mu > 10$, the changes in crystallite dimensions and % crystallinity are due to conversion from a lamellar to a fibrillar structure. They claim that the increase in TSL intensity is due to an increase in trap concentration, which in turn results from a straightening of the tie molecules running between neighbouring crystallites within the fibrils. Increases in the TSL intensity and the elastic modulus are certainly correlated $\mu$-wise, and decreases in both are correlated with respect to annealing temperature. However it is not clear why straightening of tie molecules should increase the trap concentration.

(b) Liu *et al.* [35] studied the effects of annealing and drawing on poly(ethylene terephthalete) films. Figure 7 shows several glow-curves for a sample X-irradiated in air at room temperature, one with the sample in its original condition and the others after annealing for various times at 453K in vacuum. The changes in glow-curve profile mirrored those in % crystallinity, in the sense that the % crystallinity increased from 12% to 48% after a 1 minute anneal, with little further increase on longer annealing. Drawing in water at 353K, up to a draw ratio of 5, increased the % crystallinity only from 12% to 14%; the glow-curve profile after irradiation at room temperature did not alter, but the total light output increased by 70% at a draw ratio of 5. The authors suggest that the lower temperature peak in Fig. 7 is triggered by the glass transition in the amorphous regions, the additional peak appearing after annealing originating in release of electrons from traps formed either on the newly-created crystallite surfaces or in adjacent amorphous regions. One might expect that, for the same irradiation dose, the intensity of the lower peak would decrease due to competition from the new traps. The authors speculate that "relaxation" of the amorphous state as a result of annealing enhances the efficiency of the TSL emission process, but do not offer any justification. The absence of a peak around 363K after

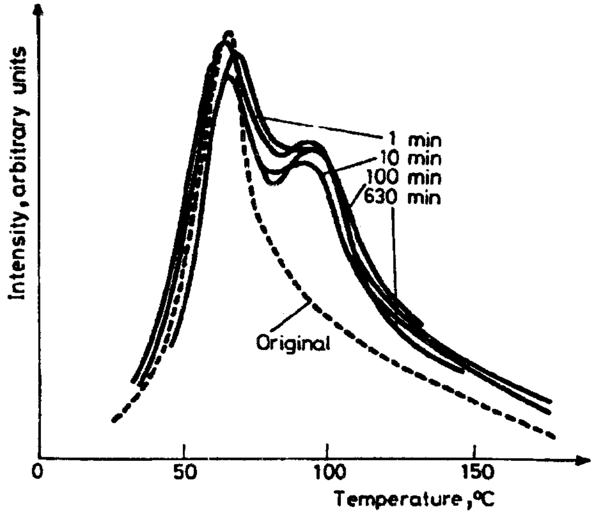

Fig. 7 TSL glow-curves for a poly(ethylene terephthalete) sample X-irradiated in air at room temperature, and then annealed for various times in vacuum at 453K [35]

drawing is consistent with a very small increase in % crystallinity, but the 70% increase in the area under the glow-curve contrasts strongly with the very small change in the first peak after annealing. If annealing enhances the TSL efficiency, as suggested by the authors, then one might expect drawing to decrease it.

(c) Markiewicz and Fleming [6] investigated the effects of morphological changes on the TSL of commercial low density polyethylene. Figure 8 shows a series of glow-curves obtained from a sample after it had been held at the indicated temperatures for 5 minutes in vacuum. Absorbed gas had first been removed from the sample by pumping, and it was X-irradiated at liquid nitrogen temperature before each glow-curve was recorded. Peak I disappeared completely after 5 minutes at 363K. The suggested explanation is that the peak I traps are cavity traps formed in the chain-fold regions, and that the chain configurations in these regions are very sensitive to heating above about 313K, when the % crystallinity begins to decrease [36]. The changes in peaks I, II and III after holding for 5 minutes at 363K were stable for at least 7 days, provided the sample was maintained in vacuum. Further heating brought about a partial re-appearance of peak I and increases in the intensities of the other two peaks. Clearly the peak heights and peak I temperature are very sensitive to the thermal history of the sample when heated above 313K; this contrasts with a reproducibility of +/- 10% in peak

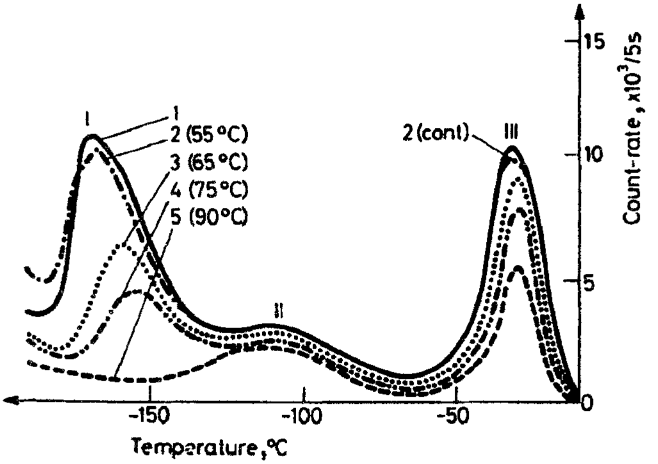

Fig. 8 TSL glow-curves for low density polyethylene samples gamma-irradiated in vacuum at liquid nitrogen temperature after removal of adsorbed air [6]: 1.without further heat treatment; 2-5 after holding for 5 minutes at the temperatures indicated

heights and +/- 5K in peak I temperature between successive glow-curves recorded without annealing.

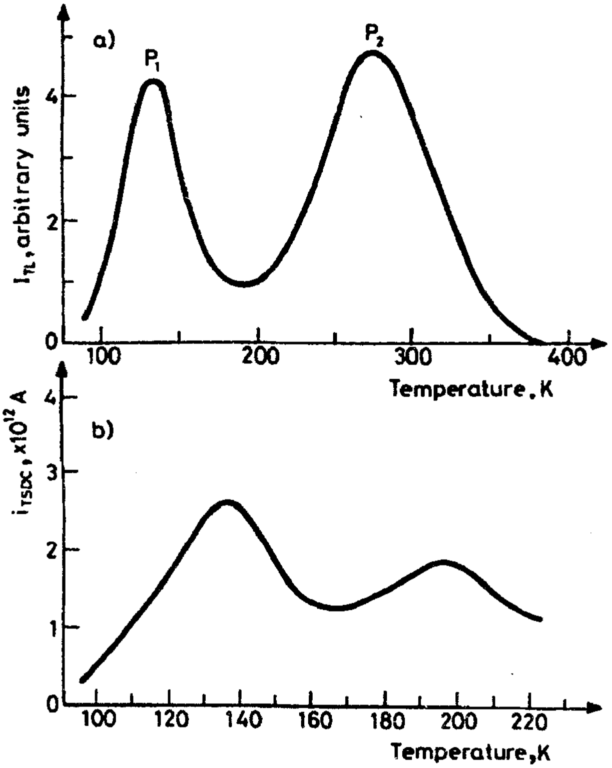

Fig. 9 (a) TSL glow-curve for a polydiancarbonate sample doped with methyl violet and uv-irradiated at 77K in vacuum; (b) TSD plot for an undoped polydiancarbonate sample dc-polarized for 30 mins at 320K [40]

The same authors [37] immersed a similar sample in fuming nitric acid for 52 hours at room temperature. No physical changes were visible to the naked eye, but no TSL was recorded immediately after immersion or after heating to 393K in vacuum. Nitric acid first "digests" the amorphous regions (including the chain-fold regions believed to contain the electron traps), and then starts to degrade the surfaces of the crystalline lamellae at a much slower rate. The largely unconnected lamellae then consist of relatively short paraffinic chains terminated at both ends by carboxyl groups [38, 39]. These chains do not re-form folded regions even after the sample is melted, and so TSL is not observed because there are no electron traps. Although nitration of the luminescence centres (e.g. anthracene, naphthalene and benzoic acid) probably results from the immersion in nitric acid, it seems unlikely that TSL would thereby be totally suppressed.

(d) Vanderschueren *et al.*[40] doped polydiancarbonate with triphenyl methane and xanthene dyes up to a level not exceeding 0.1% by weight. TSL was observed up to about 375K from samples uv-irradiated at 77K. They also made TSD measurements in a separate cell on samples of the same thickness but larger cross-section, polarising at 320K and heating from 77K. A typical TSL glow-curve and a typical TSD current plot are shown in Fig. 9 (a) and (b) respectively. Negligible TSL was observed in undoped samples, and each of six samples doped with different dyes yielded the same glow-curve profile but with varying intensities. On the other hand, doping had very little effect on either the profile of the TSD plot or the current magnitude. Note that although TSL was observed up to 375K, the TSD current was apparently too small to measure above 230K. The lower and upper temperature peaks in the TSD plot are thought to originate in re-orientation of dipoles on carbonate and carbonate/phenylene groups respectively. It seems unlikely that the TSL emission in the range 100-230K is initiated by the same dipole re-orientation, since (i) the TSD plot contains two maxima and the TSL glow-curve only one, and (ii) the two activation energy distributions, measured by the initial rise method, differ considerably. The authors suggest that the luminescence centres associated with the $P_1$ TSL peak are ionized dye molecules, with which the electrons recombine by tunneling through potential barriers, but they do not offer any justification. The origin of the $P_2$ peak is also uncertain, no intrinsic relaxation of the polymer matrix being known in the appropriate temperature range. It did not appear with every dopant, nor after X- or gamma-irradiation. Perhaps the most important point to note is that, for this particular system, it seems that the escape of electrons from traps is not driven by intrinsic molecular motion within the polymer chains, contrary to the correlations of this type described earlier. Rather the glow-curve profile seems to be characteristic of the polymer-dopant combination.

### *TSD/TSC*

(a) Belana *et al.* [41] used TSD to study the cold crystallization of amorphous poly(ethylene terephthalate) samples. They observed the evolution of the $\alpha$- and $\rho$ peaks as a function of polarization temperature (see Fig. 10), and also as a function of the maximum temperature to which the sample was heated prior to polarization at a constant (lower) temperature (see Fig. 11).

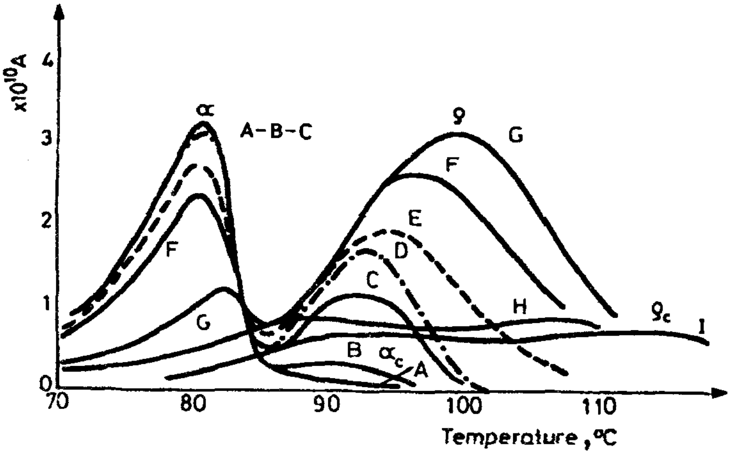

Fig. 10 TSD plots for amorphous poly(ethylene terephthalate) samples polarized at different temperatures (°C) as follows; A 75, B 80, C 85, D 90, E 100, F 110, G 118, H 122, I 130 [41]

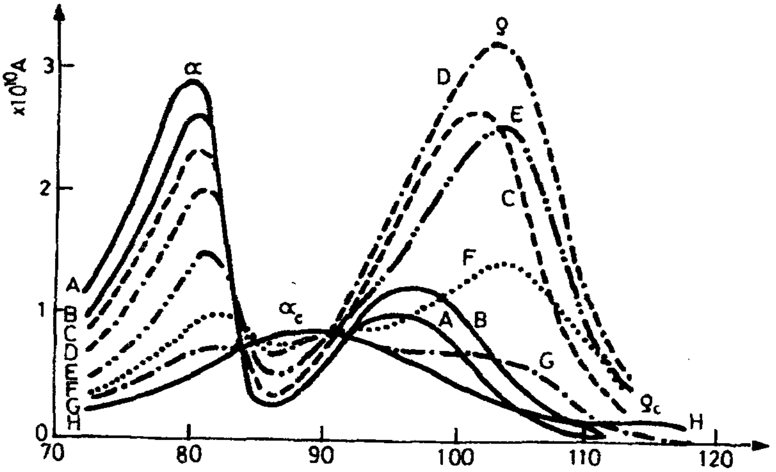

Fig. 11 TSD plots for poly(ethylene terephthalate) samples heated to successively higher final temperatures $T_f$ and then polarized at 90°C. $T_f$(°C) values were as follows; A 112, B 116.5, C 117.5, D 121, E 122, F 122.5, G 123, H 130, [41]

Figure 12 shows the % crystallinity (determined using a density gradient column) also as a function of the maximum temperature to which the sample was heated prior to polarization. The authors delineate three % crystallinity ranges as follows:-

(1) Less than 3% (Stage 1), when the $\alpha$-peak current and temperature are constant but the $\rho$-peak grows and moves towards higher temperatures.

(2) Between 3% and 30% (Stage 2), when the $\alpha$-peak current decreases but its temperature increases, while the $\rho$-peak current reaches a maximum and its temperature continues to increase.

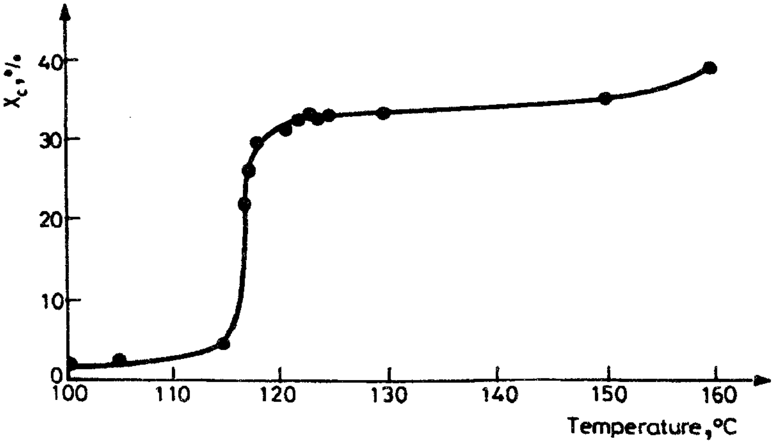

Fig. 12 Percentage crystallinity $x_c$ versus final heating temperature $T_f$ for poly(ethylene terephthalate) samples [41]

(3) Between 30% and approximately 38% (Stage 3), when the $\alpha$-peak current falls rapidly and its temperature continues to increase, and the $\rho$-peak falls rapidly at constant temperature. The $\alpha$- and $\rho$-peaks are replaced by the $\alpha_c$ and $\rho_c$ peaks in samples with crystallinities near 38%; higher crystallinities were not investigated.

As in poly(methyl methacrylate) (Fig.3), the $\alpha$-peak is dipolar in origin and is associated with the glass transition, while the $\rho$-peak originates in space charge motion. Belana *et al.* [41] attribute the increase in the $\rho$-peak during Stage 1 to the detrapping of space charge as a result of the formation of a few additional small spherulites, and the increase in peak temperature to the thermal break-up of shallower traps before deeper traps (this is perhaps questionable). However they do not specify whether the charge is electronic or ionic, and do not explain why it is present in the samples. During Stage 2 the formation of many more small spherulites causes increased hindrance to chain motion in the amorphous regions, and hence a decrease in the $\alpha$-peak current and an increase in its temperature. Simultaneously the release of more charge (on the formation of more spherulites) causes a large increase in the $\rho$-peak. In Stage 3 the additional small spherulites begin to grow, the resulting further suppression of chain motion leading to the disappearance of the $\alpha$-peak. The disappearance of the $\rho$-peak is attributed to low mobility of the space charge within the enlarged spherulites.

As stated above, in samples with crystallinities approaching 38% the $\alpha$- and $\rho$-peaks are replaced by the $\alpha_C$- and $\rho_C$-peaks. The temperatures of the latter are close to those which would be expected from extrapolation of the $\alpha$- and $\rho$-peak temperatures, suggesting a common origin for $\alpha/\alpha_C$ and $\rho/\rho_C$. However, Belana *et al.* [41] observed all four peaks simultaneously in a sample which had been polarized at 90° and then heated to 135°, and therefore concluded that they had separate origins.

(b) The work discussed next involved what are commonly called air-gap TSC measurements, in which the sample carries only one evaporated electrode, and is charged by exposure of the non-electroded surface to an electron beam or corona discharge. The electron/ion energies are usually such that the charge carriers penetrate only a small fraction of the sample thickness. On heating the sample one measures the current flowing to ground from a solid metallic electrode located close to, but not in direct contact with, the unelectroded surface; this current originates in (i) movement of charge injected from the grounded evaporated electrode, which neutralizes the charge just below the unelectroded surface either by recombining with it or being colocated with it, or (ii) release of the corona charge from traps and return to the non-electroded surface.

Baba and Ikezaki [42] compared air-gap TSC measurements on $20\mu$m thick undrawn isotactic polypropylene samples, which had been subjected to annealing treatment after electrode evaporation, with the corresponding measurements when the annealing preceded the electrode evaporation. They concluded that heat introduced into the sample during electrode evaporation, mainly the heat of condensation of the metallic vapour, changed the morphology of the volume just below the electrode and therefore also changed its trapping parameters. On comparing the TSC plots for Al, Au, Ag and Bi evaporated electrodes they also concluded that the thermally-induced changes were independent of work-function differences between the electrode and the polymer.

Ikezaki [43] also made air-gap TSC measurements on 13 $\mu$m thick fluorinated ethylene-propylene copolymer (Teflon-FEP Type A, Dupont de Nemours) samples carrying one Al electrode, either vacuum-evaporated or dc magnetron sputtered. The samples were charged at room temperature by exposing the non-electroded surface to a corona discharge in air for 3 minutes. Since the kinetic energies of sputtered metallic particles are 10-100 times greater than those of their evaporated counterparts, one expects to see much more marked localized thermal effects in samples with sputtered electrodes. Figure 13 shows air-gap TSC plots for two positively charged samples, one carrying a sputtered and the other a vacuum-evaporated Al

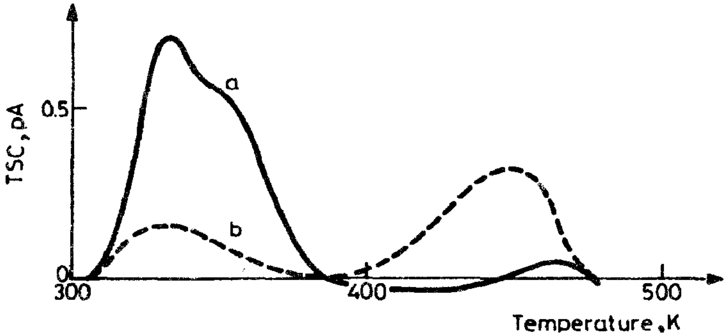

**Fig. 13** Air-gap TSD plots for positively charged fluorinated ethylene-propylene (FEP) co-polymer samles with (a) a magnetron sputtered aluminium electrode, (b) a vacuum-evaporated aluminium electrode. The initial potential of the charged surface magnetron was (a) 229V, (b) 236V [43]

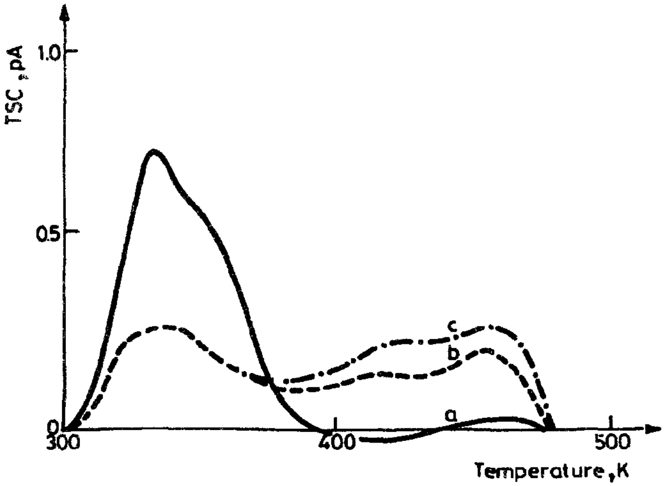

**Fig. 14** Effect of annealing on air-gap TSD measurements of positively charged fluorinated ethylene-propylene (FEP) samples with a magnetron sputtered aluminium electrode; (a) first run, (b) second run, (c) trird run. The initial potential of the charged surface was (a) 229V, (b) 227V, (c) 229V [43]

electrode. The two differ considerably, reflecting different trapping parameters for charge injected into the sample volume just below the electrode. Figure 14 shows the changes in the TSC current profile resulting from repeated runs on a positively-charged sample with a sputtered electrode. In effect the sample is annealed during each run, and one therefore expects the profile to change, at least between the first few runs. It will be seen that the low temperature peak stabilizes after the second run, but the higher temperature features do not. The complete current profile for a negatively-charged sample heated to a slightly higher temperature was found to be stable after the second run, suggesting that positive charge traps are annealed at lower temperatures than their negative counterparts. These experiments show the considerable sensitivity of the TSC technique to the thermal history of the sample.

(c) Markiewicz and Fleming [9] made simultaneous TSL/TSC measurements on thin film samples of commercial low density polyethylene after they had been subjected to various treatments which affected their morphology. (The TSL data of the same authors [6, 37] discussed above relates to 1.8 mm thick samples on which TSC measurements would have been very difficult.) The samples were polarized at 20° for 5 minutes at a field strength of 90 kV/cm, and X-irradiated at liquid nitrogen temperature with the field applied. Figure 15 shows the effects of immersion in fuming nitric acid on the TSC plots; curve A is for an untreated sample, and curves B, C and D after 22 hours, 65

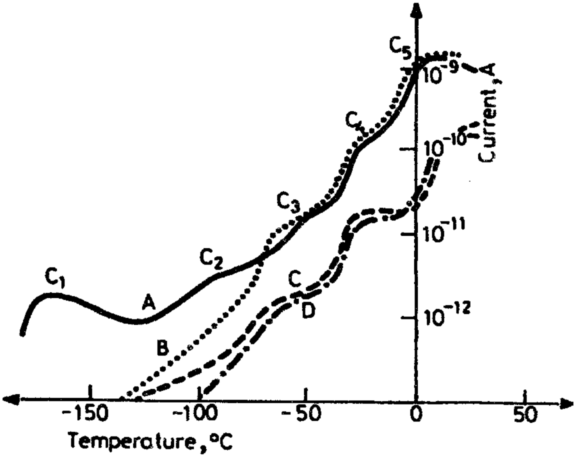

Fig. 15 Effects of immersion in fuming nitric acid at room temperature on the TSC of a low density polyethylene sample [9]

hours and 45 days immersion respectively. Note the early disappearance of peaks $C_1$ and $C_2$, and the absence of significant changes to peaks $C_3$, $C_4$ and $C_5$ after an initial reduction. The TSL was barely detectable after 22 hours immersion, and the % crystallinity decreased from 41% initially to 38% after 45 days immersion. Figure 16 shows the effects of holding a sample for 16 hours in vacuum at 100° in open circuit. The TSC current (lower plot) fell by approximately a factor of 10 in the $C_1$-$C_2$ peak region, and the current profile at higher temperatures was considerably altered. The TSL intensity (upper plot) decreased by approximately 50% and the % crystallinity increased from 41% to 45%, as a result of this treatment.

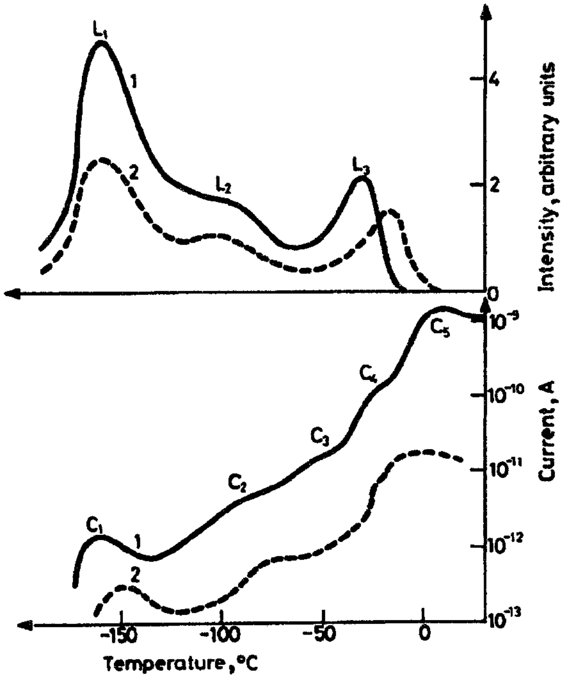

Fig. 16 Effects of annealing at 100oC in vacuum on the TSL (upper plot) and TSC (lower plot) of a low density polyethylene sample [9]

The effect of absorbed gases on the TSC/TSL signals is shown in Fig. 17. Well-defined "gas" peaks, labelled $C_g$ and $L_g$ in the TSC and TSL plots respectively, disappeared when absorbed gases were removed, and the $C_1$, $C_2$ and $L_2$ peaks became clearly visible. Note that the $C_3$, $C_4$ and $C_5$ TSC peaks were unaffected by the gas removal.

The main conclusions drawn from these results were as follows:-

(1) Electrons are released from the same traps (formed by the polymer chain configurations in the chain-fold regions of the samples) to generate the $L_1$ and $C_1$ peaks. The same is true of the $L_2$ and $C_2$ peaks. In both cases the release is triggered by molecular chain motion. The chain configurations are sensitive to annealing well above the glass transition temperature.

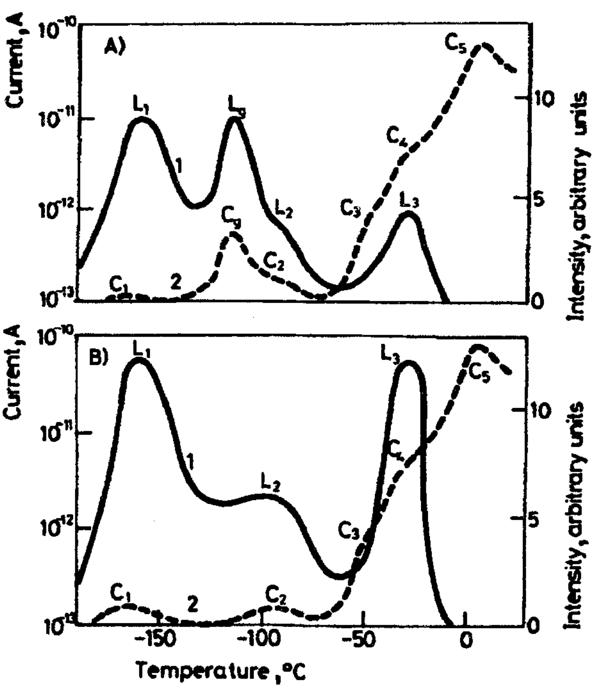

**Fig. 17** Effects of adsorbed air on the TSL and TSC of low density polyethylene. Samples irradiated and heated (A) in the presence of adsorbed air, (B) after pumping out adsorbed air [9]

(2) The traps associated with the $C_3$, $C_4$ and $C_5$ TSC peaks are structural defects in the crystalline regions, from which the electrons escape by thermal excitation. These traps are largely unaffected by immersion of the samples in nitric acid, because the crystalline regions are almost totally impermeable to liquids, but they are sensitive to annealing.

(3) The same traps are associated with the $C_g/L_g$ peaks, and the $C_1/L_1$ and $C_2/L_2$ traps "compete" with the gas traps for electron capture.

## Conclusion

It will be clear that TSL and TSD/TSC are extremely sensitive non-destructive monitors of charge trapping and transport in organic polymers, and therefore of the recent thermal history of the sample. Since unlike conventional thermal analysis measurements they are interpreted at the molecular/electronic level, but like the latter are relatively quickly and inexpensively carried out, it is suggested that it would be advantageous to perform both, possibly simultaneously. Neither is an exact science, but taking them together will certainly enable a more exact interpretation of both!

* * *

This review was written during my stay at the Institute for Molecular Science as Visiting Professor. I wish to thank Professors Y. Maruyama and H. Inokuchi for their thoughtful hospitality, and the Japanese Ministry of Education Science and Culture for financial assistance.

## References

1 C. B. Murphy, in Differential Thermal Analysis, ed. R. C. Mackenzie, Academic Press, 1970, Vol.1, Ch.23.
2 Thermal Analysis in Polymer Characterization, ed. E. A. Turi, Heyden & Son Inc., Philadelphia 1981.
3 J. Paulik, F. Paulik and M. Arnold, J. Thermal. Anal., 32 (1987) 301.
4 A. M. Kaplan, A. P. Shvedchikov, S. V. Lotnik and V. P. Kazakov, Proc. 8th Int. Congress Thermal Anal., ed. Blazek, Alfa: Bratislava, Czechoslovakia, 1985, pp.303-304
5 R. J. Fleming and J. Hagekyriakou, Radiation Protection Dosimetry, 8 (1984) 99.
6 A. Markiewicz and R. J. Fleming, J. Polymer Sci. Part B: Polymer Physics, 24 (1986) 1713.
7 J. Vanderschueren and J. Gasiot, in Thermally Stimulated Relaxation in Solids, ed. P. Braunlich, Topics in Applied Physics (Springer-Verlag), 37 (1979) Ch.4.
8 J. van Turnhout, in Electrets, ed. G. M. Sessler, Topics in Applied Physics (Springer-Verlag), 33 (1980) Ch.3.
9 A. Markiewicz and R. J. Fleming, J. Phys. D: Appl. Phys. 21 (1988) 349.
10 L. A. DeWerd in Thermally Stimulated Relaxation in Solids, ed. P. Braunlich, Topics in Applied Physics (Springer-Verlag) 37 (1979) Ch.6.
11 G. M. Sessler and J. E. West, in Electrets, ed. G. M. Sessler, Topics in Applied Physics (Springer-Verlag) 33 (1980) Ch.7.
12 R. H. Partridge, J. Polymer Sci. Part A, 3 (1965) 2817.
13 D. J. Morantz and C. S. Bilen, Polymer(UK), 16 (1975) 745.
14 C. David, P. Janssen and G. Geuskens, Int. J. Radiat. Phys. Chem. 4 (1972) 51.
15 J. Hagekyriakou and R. J. Fleming, J. Phys. D: Appl. Phys. 15 (1982) 1795.
16 J. T. Randall and M. H. F. Wilkins, Proc. Roy. Soc. A184 (1945) 366.

17 R. Chen and Y. Kirsh, Analysis of Thermally Stimulated Processses, Pergamon Press, 1981.
18 L. F. Pender and R. J. Fleming, J. Phys. C: Solid State Phys. 10 (1977) 1571.
19 R. A.Creswell and M. M. Perlman, J. Appl. Phys. 41 (1970) 2365.
20 Y. Hama, Y. Kimura, M. Tsumura and N. Omi, Chem. Phys. 53 (1980) 115.
21 A. Charlesby and G. P. Owen, Int. J. Radiat. Phys. Chem. 8 (1976) 343.
22 A. Charlesby, Int. J. Radiat. Phys. Chem. 17 (1981) 399.
23 A. Bernes, R. F. Boyer, D. Chatain. C. Lacabanne and J. P. Ibar, in Order in the Amorphous State of Polymers, ed. S. E. Keinath, R. L. Miller and J. K. Rieke, Plenum Publishing Corporation, 1987, p. 305.
24 M. L. Williams, R. F. Landel and J. D. Ferry, J. Amer. Chem. Soc. 77 (1955) 3701.
25 M. L. Williams, J. Phys. Chem. 59 (1955) 95.
26 L. Zlatkevich, Radiothermoluminescence and Transitions in Polymers, Springer-Verlag 1987, Ch.1 and 2.
27 I. Boustead, Eur. Polymer J. 6 (1970) 731.
28 A. G. Perekupka and V. A. Aulov, Vysokomol. Soedin (Series B), 22 (1980) 583.
29 A. G. Perekupka and V. A. Aulov, Vysokomol. Soedin (Series B), 22 (1980) 578.
30 A. G. Perekupka and V. A. Aulov, Dokl. Akad. Nauk. SSSR (Phys. Chem.), 247 (1979) 1408.
31 A. Charlesby and R. H. Partridge, Proc. Roy. Soc. A283 (1965) 312.
32 I. Boustead and A. Charlesby, Eur. Polymer J. 3 (1967) 459.
33 N. S. Allen, J. Homer, J. F. McKellar and D. G. M. Wood, J. Appl. Polymer Sci. 21 (1977) 3147.
34 V. A. Aulov, Yu. A. Zubov and N. F. Bakayev, Polymer Sci. U.S.S.R. 27 (1985) 1305.
35 L. B. Liu, K. Hiyama and K. Miyasaka, Polymer(UK), 29 (1988) 286.
36 W. L. Hawkins, Polymer Degradation and Stabilization (Springer, Berlin) 1984, p. 15.
37 A. Markiewicz and R. J. Fleming, J. Polymer Sci. Part B: Polymer Phys, 25 (1987) 1885.
38 A. Keller and Y. Udagawa, J. Polymer Sci. Part A-2, 9 (1971) 1793.
39 M. E. Cagiao, D. R. Rueda and F. J. Balta Calleja, Colloid Polymer Sci. 261 (1983) 626.
40 J. Vanderschueren, A. Linkens and J. Niezette, J. Polymer Sci. Part B: Polymer Phys. 25 (1987) 1537.
41 J. Belana, M. Pujal, P. Colomer and S. Montserrat, Polymer(UK), 29 (1988) 1738.
42 A. Baba and K. Ikezaki, J. Appl. Phys. 57 (1985) 359.
43 K. Ikezaki, phys.stat.sol.(a) 103 (1987) 481.

**Zusammenfassung** - Es werden diejenigen physikalischen Erscheinungen umrissen, auf denen Messungen von thermisch stimulierter Lumineszenz und Leitfähigkeit basieren, die logisch als ergänzend zu herrkömmlichen thermoanalytischen Messungen betrachtet werden. Zur Durchführung von Messungen dieser Art benötigte Einrichtungen und Proben werden kurz beschrieben und Grundbegriffe für die Interpretierung der experimentellen Ergebnisse skizziert. Einige frühere experimentelle Daten, die ausgewählt wurden, um die Empfindlichkeit der thermisch stimultierten Lumineszenz und Leitfähigkeit gegenüber Dopen der Probe bzw. Vernäderungen in ihrer Morphologie zu verdeutlichen, werden vorgestellt und diskutiert.